Effect of solution temperature on aging behavior and properties of SiC$_p$/Al–Cu–Mg composites

P. Jin, B.L. Xiao, Q.Z. Wang, Z.Y. Ma[*], Y. Liu[1], S. Li

Shenyang National Laboratory for Materials Science, Institute of Metal Research, Chinese Academy of Sciences, 72 Wenhua Road, Shenyang 110016, China

ABSTRACT

In this study, the effect of solution temperature on artificial aging kinetics of 15 vol.% SiC particles reinforced 2009Al (SiC$_p$/2009Al) composite prepared using a powder metallurgy method was investigated by means of microstructural examinations, hardness measurement and DSC analyses. The study indicated that, with increasing the solution temperature from 495 to 560 °C, while the GP zone formation and dissolution were retarded due to the decreased quenched-in vacancy concentration, the S′ precipitation was promoted due to the increased dislocation density. This accelerated the aging kinetics of the composite with increasing the solution temperature from 495 to 560 °C. Furthermore, the composite which was solutionized at 530 °C exhibited the highest peak hardness and tensile strength. The effect of the solution temperature on the aging behavior and tensile properties of the composite was explained in terms of the variation of the microstructual mechanisms.

© 2010 Elsevier B.V. All rights reserved.

1. Introduction

Discontinuously reinforced aluminum (DRA) matrix composites have received significant attention in recent years. The high specific strength and stiffness make the DRA composites attractive as candidate materials for aerospace and automotive applications [1–3]. The investigations of ceramic particle reinforced aluminum matrix composites have revealed that the presence of the reinforcing particles in the aluminum matrix usually does not alter the aging sequence of the aluminum alloys, but changes the precipitation kinetics significantly [4–11].

Thomas and King [9] found that the SiC$_p$/2124Al composite exhibited an accelerated aging phenomenon compared to the unreinforced alloy, due to the enhanced S′ (Al$_2$CuMg) phase formation. This is attributed to the presence of a high density of dislocations. Suresh et al. [12] also reported that the addition of SiC particles in Al–3.5 wt.%Cu accelerated the aging kinetics. The large difference in the coefficient of thermal expansion (CTE) between the aluminum matrix and the ceramic reinforcement causes differential strain at the reinforcement/matrix interface during quenching, with plastic relaxation leading to the generation of dislocations [13]. Although the high density of dislocations would inhibit the formation of GP zones, it would increase the nucleation rate and growth rate of the precipitates such as the S′ phase through enhanced dislocation-

assisted diffusion [6,9,14], thereby accelerating the aging kinetics of the composites.

However, different age-hardening behaviors were also reported in the DRA composites. Kim et al. [15] reported a significant retardation in the age-hardening kinetics (i.e. prolonged time to reach peak hardness) for SiC$_p$/Al–4 wt.%Cu composites. Song et al. [16] found that the SiC addition into the Al–Zn–Mg–Cu alloy decelerated the aging kinetics, due to the depletion of Mg in the matrix and the lack of interaction between the Zn and the dislocations. Similarly, Pal et al. [17] revealed that it took a longer time for the composites to reach the peak aging than the unreinforced alloy. They attributed this behavior to the lower vacancy concentration, the large-scale interfacial segregation of the alloying elements and inadequate dislocation density. It is believed that the nature of change in the age-hardening kinetics during aging of the composites depends on the matrix material, reinforcing particulates such as size, morphology and volume fraction, composite processing route, solution and aging temperatures, etc. [17].

While the aging kinetics of the composites has been widely investigated [9,18–21], the effect of solution-treatment temperature on the aging behavior of the SiC$_p$/Al composites was hardly studied [17]. In some previous studies, it was reported that the increases in the solution temperature could increase the strength and elongation of SiC whiskers or particles reinforced 2xxx aluminum alloy composites fabricated by a powder metallurgy (PM) technique [22,23]. However, these studies did not focus on the role of the solution temperature in the aging process of the composites.

Considering that the variation in the solution temperature might change the quenched-in vacancy concentration, dislocation den-

* Corresponding author. Tel.: +86 24 83978908; fax: +86 24 83978908.
E-mail address: zyma@imr.ac.cn (Z.Y. Ma).
[1] Now is with Northeastern University, Shenyang 110004, China.
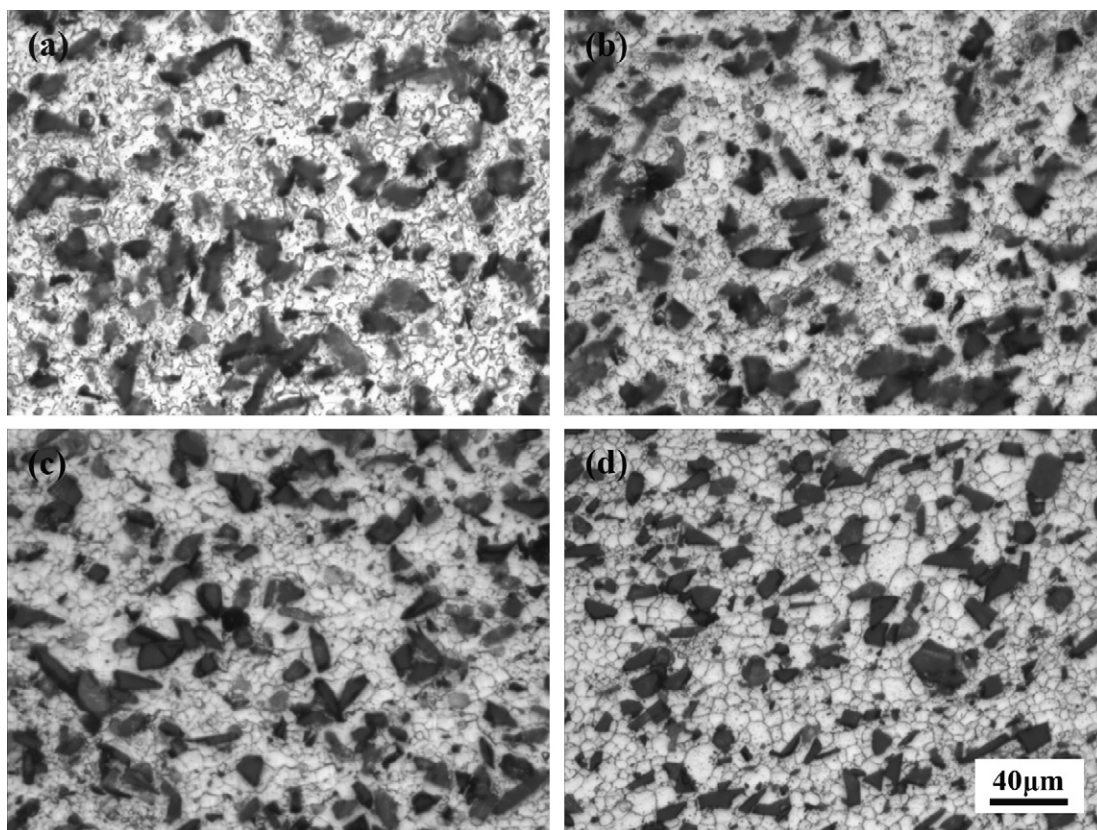
Fig. 1. Optical micrographs of SiC$_p$/2009Al composites in the transverse direction: (a) extruded, (b)–(d) solution treated at (b) 495 °C, (c) 530 °C, and (d) 560 °C.

sity and second-phase dissolution, it is of practical importance to understand the effect of the solution-treatment temperature on the aging behavior of the SiC$_p$/Al composites. In this study, a 15 vol.%SiC$_p$/2009Al composite produced using the PM technique was subjected to solution-treatment at different temperatures and then a subsequent aging. The aging behavior was examined by means of the Vickers hardness tests and DSC analyses. The aim is to understand the effect of the solution-treatment temperature on the aging behavior of the SiC$_p$/Al composites.

2. Experimental

2009Al alloy and 15 vol.%SiC$_p$/2009Al composite were used in this study. 2009Al has a nominal composition of Al–3.7Cu–1.3Mg (wt.%). The SiC particles were irregularly shaped, with a nominal particle size of 7 μm. The composite was fabricated by the PM process and a subsequent extrusion. The Al and SiC powders were blended for 8 h and then compacted with a single-action, uniaxial hydraulic press at a pressure of 150 MPa. The compacts were sintered at 580 °C for 1 h and then extruded at 480 °C at an extrusion ratio of 10:1. The as-extruded composite was solution treated at 495 °C, 530 °C and 560 °C for 1 h, water quenched, and then aged at 175 °C for various periods up to 200 h. For comparison, the unreinforced matrix alloy was also fabricated and treated under the same conditions.

The specimens for microstructural examinations were machined perpendicular and parallel to the extrusion direction. The specimens were ground with a 2000 grit abrasive paper and then mechanically polished. In order to reveal the grain size, the polished specimens were etched with Keller's reagent. The specimens were observed using an optical microscope (OM) and a scanning electron microscope (SEM, HITACHI S-3400N). The precipitates in the composites receiving different treatments were

examined using a transmission electron microscope (TEM, TECNAI G^2). The thin films for TEM were prepared using the ion-milling technique.

The age hardening responses of the composite and the unreinforced matrix alloy were characterized using Vickers micro-hardness measurement. The tests were performed on a FM-700 tester with the load of 20 kg and a loading time of 15 s. Five measurements per condition ensured the accuracy of results. Tensile test was performed at a crosshead speed of 1 mm/min using an Instron 100 kN screw-driven machine. The tensile specimens with a gage diameter of 5 mm and a gage length of 25 mm were machined from the as-extruded bar with the loading axis parallel to the extrusion direction. The specimens were heat treated prior to machining to prevent specimen distortion during the heat treatment.

Small slices (approximately 5 mm × 10 mm and 1–1.2 mm thick) were cut from the extruded bar. The slices were solutionized at different temperatures for 1 h and water quenched. The slices were ground with a 1200 grit abrasive paper and then cut into 3 mm × 3 mm square samples. The DSC tests were conducted on each sample in the as-quenched condition using a Mettler TA Q1000 thermal analyzer. A range of heating rates (from 5 to 30 °C/min) was used. At least two samples in each solution condition were used for each heating rate and the results obtained were found to be reproducible. The DSC scans were initiated at 50 °C and completed at 400 °C.

3. Results and discussion

3.1. Microstructural characterization

Fig. 1 shows the micrographs of the 15 vol.%SiC$_p$/2009Al composite samples in the as-extruded and as-solutionized conditions
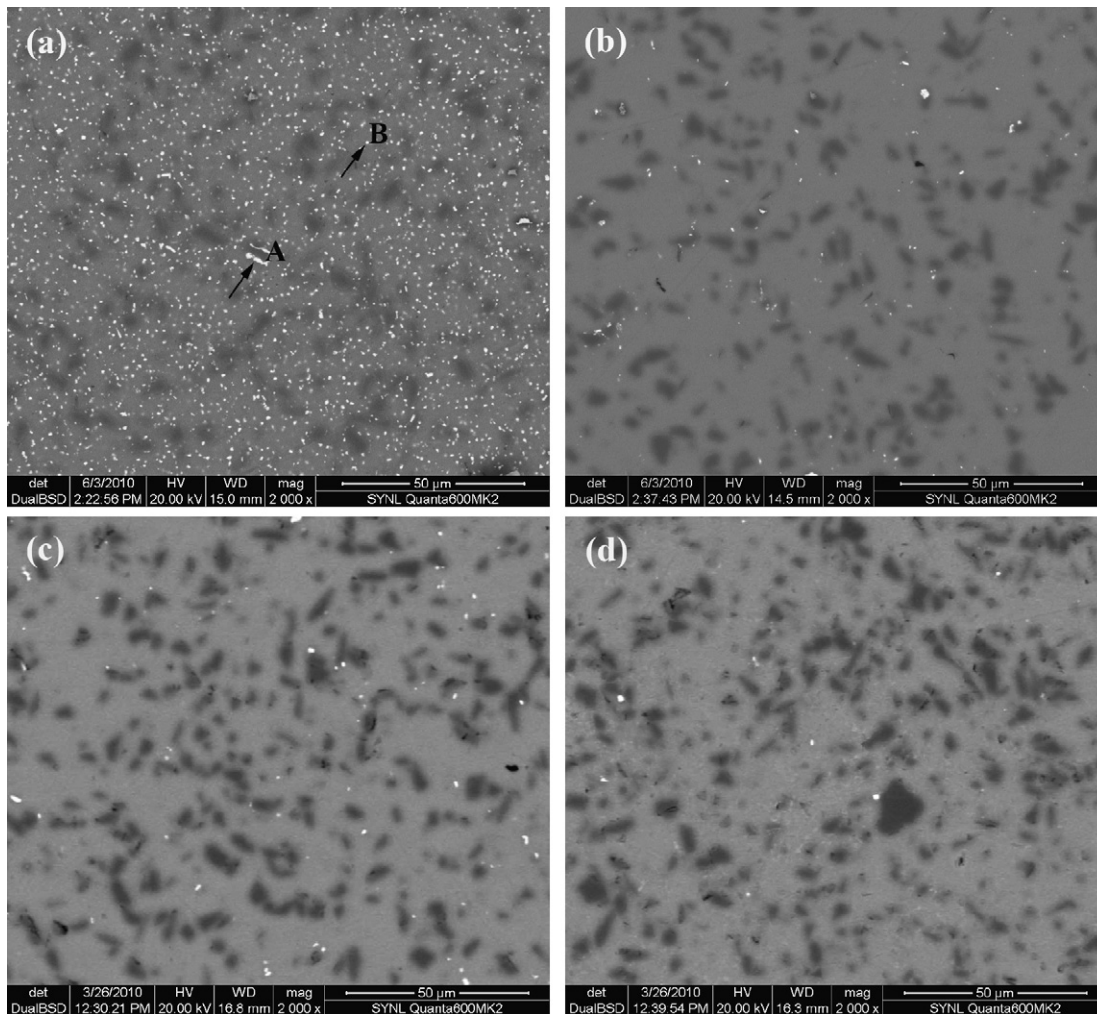
Fig. 2. SEM micrographs of $SiC_p/2009Al$ composites: (a) extruded, (b)–(d) solution treated at (b) 495 °C, (c) 530 °C, and (d) 560 °C.

with different solution temperatures. For all the composite samples, the SiC particles exhibited a uniform distribution. While it appears that the solution treatment at 495 °C did not coarsen the grain size of the matrix considerably, the grain size increased evidently with increasing the solution temperature from 495 to 560 °C, as shown in Figs. 1b–d.

Fig. 2 shows the SEM micrographs of the 15 vol.%$SiC_p/2009Al$ composite samples in the extruded and the three different solution treatment conditions. It can be seen that there is a considerable volume fraction of second-phase particles in the as-extruded composite (Fig. 2a). The high brightness of these particles is due to the higher atomic number of Cu in comparison with that of aluminum, silicon and carbon. EDX spot analyses confirmed the enrichment of solutes, including Cu and Fe, at the bright spots, as shown in Fig. 2a. Two kinds of particles were identified by EDX analyses as shown in Fig. 3, with the compositions close to those of Al_2Cu (θ phase) and Al_7Cu_2Fe. The presence of the Al_2Cu and Al_7Cu_2Fe phases were further identified according to the XRD analyses, as shown in Fig. 4. The Al_2Cu precipitates were formed during slow cooling after the hot extrusion, whereas the Al_7Cu_2Fe phase was generated during the hot-pressing fabrication.

After the solution treatment at a solution temperature of 495 °C, which is normally used for 2009Al, while most of the second-phase particles disappeared, a few coarse particles could still be observed in the composite (Fig. 2b). After the solution treatment, only GP zones could be formed at room temperature, and they were
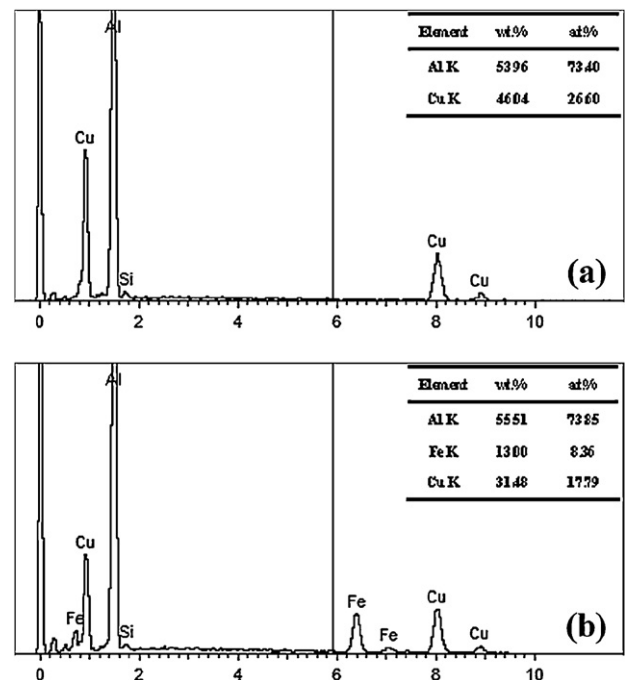

Fig. 3. EDX spectrum of particles shown in Fig. 2a: (a) spot A and (b) spot B.
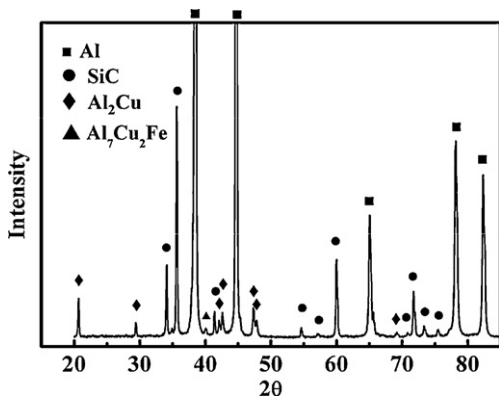
Fig. 4. XRD pattern of as-extruded 15 vol.% SiC/2009Al composite.

Table 1
A summary of peak aging hardness and peak time for unreinforced alloy and SiC$_p$/2009Al composite solutionized at different temperatures.

Solution temperature, °C	Unreinforced alloy		Composite	
	Hardness	Time, h	Hardness	Time, h
495	143.0	30	158.5	24
530	143.1	28	161.4	18
560	133.2	26	159.3	16

not discernible under SEM. So the remaining coarse particles in the solutionized composites should be undissovled second-phases. These phases were identified to be Al$_2$Cu and Al$_7$Cu$_2$Fe by the EDX analyses. This indicates that the normal solution temperature could not achieve the complete dissolution of the second-phase particles in the matrix. Increasing the solution temperature to 530 °C resulted in a decrease in the undissolved second-phase particles, Al$_2$Cu particles in particular (Fig. 2c). When the solution treatment was conducted at 560 °C, the Al$_2$Cu particles were almost completely dissolved, while some Al$_7$Cu$_2$Fe particles could be still detected in the matrix (Fig. 2d), indicating that the Al$_7$Cu$_2$Fe phase is more thermally stable than the Al$_2$Cu phase. Therefore, the solution treatment temperature has a significant effect on the dissolution of the second-phase particles, Al$_2$Cu precipitates in particular. In order to achieve a complete dissolution of the precipitates, a higher solution temperature is desired.

3.2. Aging kinetics

3.2.1. Hardness profiles

Fig. 5a–c shows the hardness changes of the composite and the unreinforced alloy as a function of aging time after the solution treatment at 495 °C, 530 °C and 560 °C, respectively. The peak hardness values and the peak aging times for both the composite and the unreinforced matrix alloy solutionized at various temperatures are summarized in Table 1. Fig. 5 and Table 1 reveal following important observations. First, the composite exhibited an apparent acceleration in aging kinetics compared to the unreinforced matrix alloy for various solution temperatures. Such an accelerated aging phenomenon is consistent with the previous reports by Thomas and King [9] and Suresh et al. [12]. The unreinforced alloy presented a broad hardness peak while the composite showed a sharp peak. Appendino et al. [8] thought that this behavior was probably due to the high dislocation density in the composite. Second, with increasing the solution temperature, both the composite and the unreinforced alloy exhibited the accelerated aging kinetics. Most noticeably, the peak aging time of the composite was shortened from 24 to 18 h with increasing the solution temperature from 495 to 530 °C. Third, increasing the solution temperature from 495 to 530 °C resulted in a slight increase in the peak hardness of the composite, but the peak hardness of the unreinforced matrix alloys did

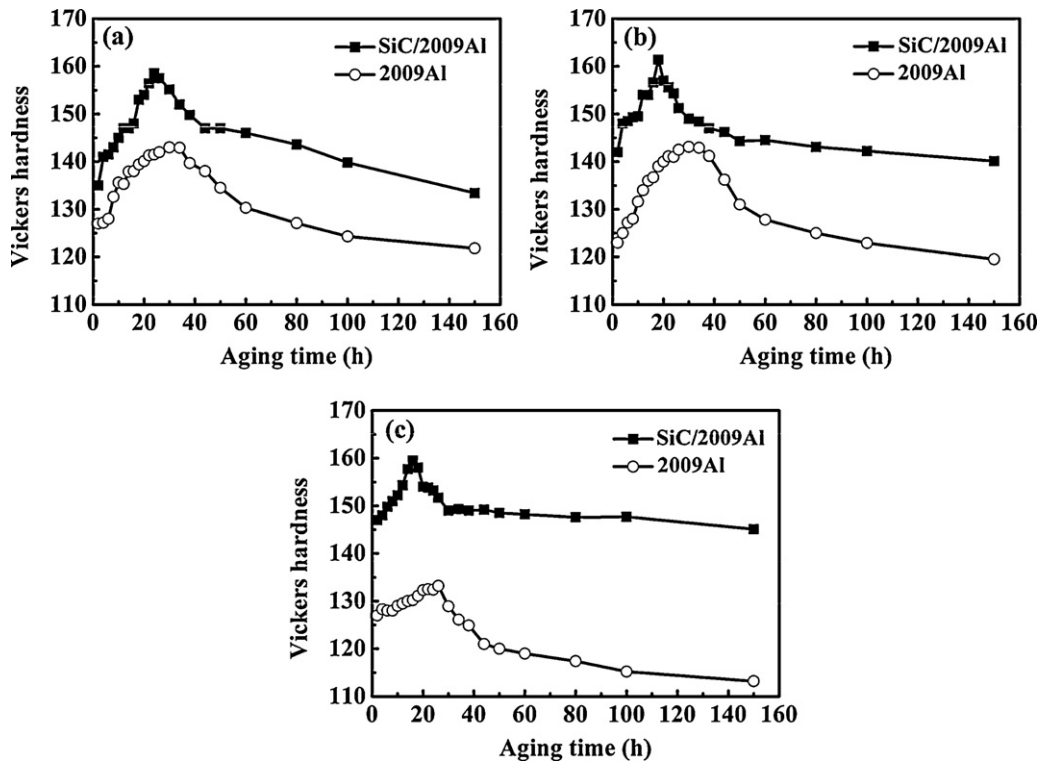**Fig. 5.** Variation of hardness with aging time for 15 vol.% SiC$_p$/2009Al composite and 2009Al alloy aged at 175 °C and solutionized at (a) 495 °C, (b) 530 °C, (c) 560 °C.
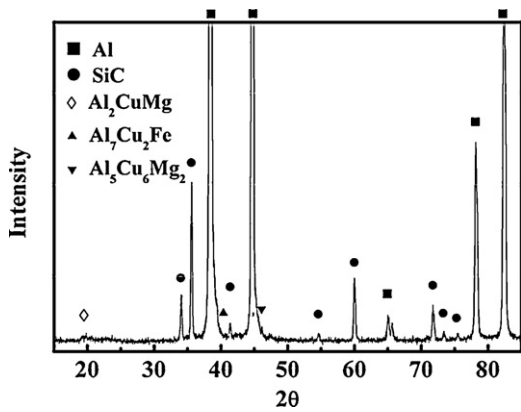
Fig. 6. XRD pattern of the composite aging at 24 h after solution treated at 530 °C.

not exhibit an increase. Further increasing the solution temperature to 560 °C caused the peak hardness of the composite to decrease to the level at 495 °C. The variation trend in the peak hardness for the present SiC$_p$/2009Al composite with the solution temperature is consistent with that in the tensile strength for SiC$_w$/2024Al and SiC$_p$/2024Al composites [22,23]. However, the unreinforced matrix alloy solution-treated at 560 °C exhibited a significantly reduced peak hardness. This might be associated with the significant grain growth. Özbek [24] found that increasing the solution temperature of 2618Al alloy to 560 °C coarsened both the grains and the precipitates, leading to a substantial reduction in the hardness.

3.2.2. Precipitate evolution

Fig. 6 shows the XRD pattern of the aged composite with the solution treatment at 530 °C. The presence of Al$_2$CuMg and

Al$_5$Cu$_6$Mg$_2$ (σ) phases are identified according to the XRD analyses. This phenomenon indicates that the strengthening phases are the Al$_2$CuMg and Al$_5$Cu$_6$Mg$_2$.

Fig. 7 shows the TEM micrographs of the composites aged at 175 °C for 24 h. Fig. 7a shows the microstructure under the peak aging condition for the composite solutionized at 495 °C. It consisted of a needle-shaped S′ phase and a cubic-shaped σ phase. A cubic σ phase was first observed in the DRA composites by Schueller et al. [25,26] in squeeze cast SiC/Al–4.3Cu–2.0Mg composite. Rodrigo et al. [27] also observed σ phase in SiC$_p$/2009Al composite. For the composite solutionized at 530 and 560 °C, the precipitates were evidently coarsened after aging at 175 °C for 24 h, indicating the occurrence of overaging (Figs. 7b and c). The TEM results are consistent with the hardness profiles (Fig. 5).

3.2.3. Thermal diffusion activation energy for precipitation

Fig. 8 shows the DSC curves of the composites solutionized at various temperatures. The curves in Fig. 8 exhibit similar heating effects, and the principal features of the curves are the three exothermic peaks A, C and D, and the sole endothermic peak B. Exothermic peak A was attributed to the formation of GP zones, endothermic peak B was associated with the dissolution of the GP zones, and exothermic peak C was ascribed to the formation of the S′ phase [18,19,28]. Exothermic peak D in Fig. 8c is different from that in Fig 8a–b, and corresponds to the formation of the θ′ (Al$_2$Cu) phase [28,29]. Fig. 8 shows that the formation and dissolution of the GP zones and the formation of the S′ phase are dominated by their reaction kinetics. The average values of the reaction peak temperatures associated with the formation and dissolution of the GP zone and the formation of the S′ phase are shown in Table 2. The peak temperatures correspond to the points of maximum enthalpy of the formation or dissolution.
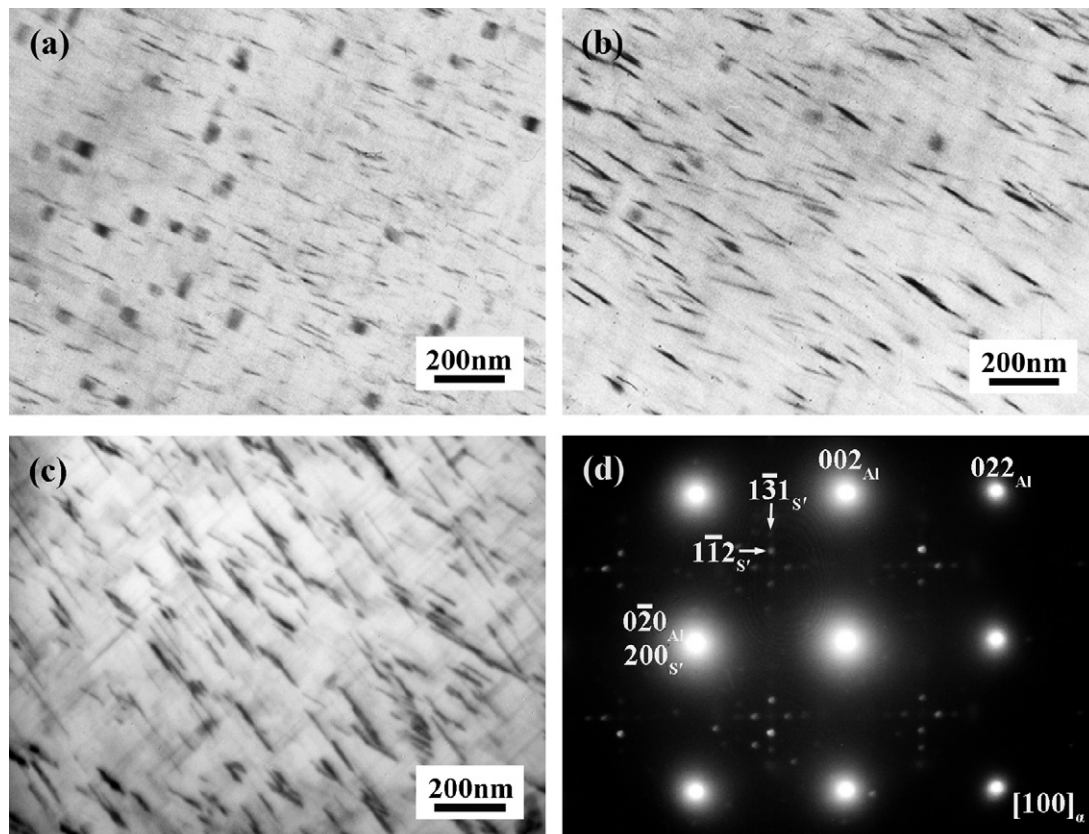

Fig. 7. TEM micrographs of the composites aging at 24 h after solution treated at (a) 495 °C, (b) 530 °C, (c) 560 °C, and (d) diffraction pattern of S′ phase.
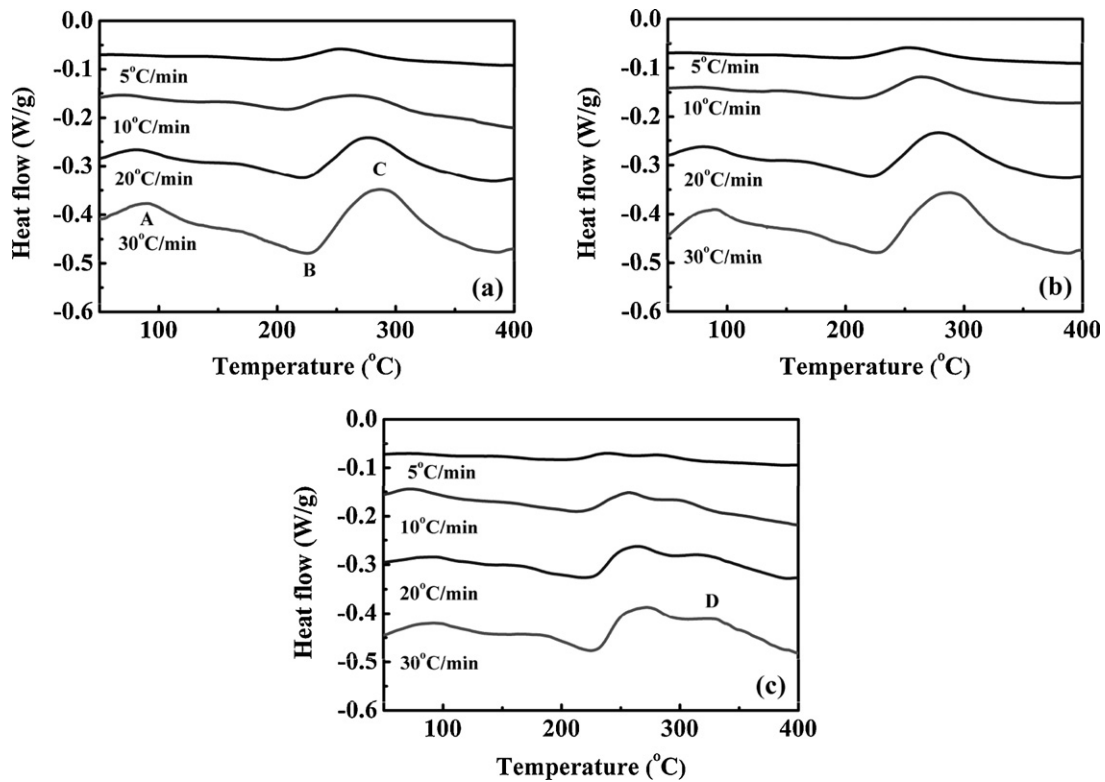
Fig. 8. DSC curves at different heating rates of SiC$_p$/2009Al composites solution treated at (a) 495 °C, (b) 530 °C, (c) 560 °C.

Thermal diffusion activation energy during the precipitation process can be calculated with the following equation [29]:

$$\ln\left(\frac{T_P^2}{\Phi}\right) = \frac{Q}{RT_P} + \ln\beta \tag{1}$$

where T_P is the peak temperature of the formation or dissolution of the precipitates, Φ is the heating rate, Q is the thermal diffusion activation energy, and R is the gas constant (8.314 J/mol), β is the state variable fully determining that fixed state of transformation. In order to estimate the thermal diffusion activation energy, the variations of $\ln[T_P^2/\Phi]$ with $1/T_P$ are plotted at different solution temperatures, and fitting the data points at different heating rates produces fitted straight lines with a slope of Q/R (Fig. 9). Then, the thermal diffusion activation energy of different precipitates can be calculated, and the results are summarized in Table 3.

The values of the activation energy for the GP zone formation obtained in the present study using the varying-heating rate

method are 49.1–60 kJ/mol for the solution temperatures from 495 to 560 °C. The migration energy of the vacancies in the Al–Cu alloys has been reported to be in the range of 41–66.9 kJ/mol [30]. The values of the activation energy for the GP zone formation obtained in this study are well within this range. With increasing the solution temperature, the activation energy for the GP zone formation increases. This phenomenon can be explained in terms of the variation in the concentration of the free vacancies required for the nucleation of the GP zones with the dislocation density.

With increasing the solution temperature, the dislocation density would increase [13]. When the composite is cooled from the solution treatment temperature, mismatch strains occur due to difference in the CTEs between the matrix and the reinforcements. The mismatch strain ε can be calculated by Arsenault and Shi [13]:

$$\varepsilon = \Delta\alpha\Delta T \tag{2}$$

where $\Delta\alpha$ is the difference in the CTEs between the matrix and the reinforcements and ΔT is the temperature change.

Because of the thermal mismatch strains, plastic deformation will take place, and this produces a high density of dislocations, especially in the vicinity of the SiC particles. The dislocation density ρ can be calculated as follows [13]:

$$\rho = \frac{BV_f\varepsilon}{bt(1-f)} \tag{3}$$

Table 2
Temperature of exothermic and endothermic peaks of the SiC$_p$/2009Al composites, solution-treated at different temperatures, at different heating rates.

Solution temperature, °C	Heating rate, °C/min	Peaks temperature, °C		
		GP formation	GP dissolution	S′ precipitation
495	5	60.8	198.9	252.3
	10	73.2	207.6	262.1
	20	80.2	221.05	276.6
	30	96.5	225.45	286.8
530	5	63.1	199.8	249.7
	10	75.8	210.4	269.9
	20	84.8	221.35	276.9
	30	89.3	226.25	286.6
560	5	64.0	199.7	237.9
	10	76.2	212.7	256.1
	20	86.3	219.1	261.3
	30	90.7	225.0	275.2

Table 3
Diffusion activation energies of SiC$_p$/2009Al composite with different solution temperatures.

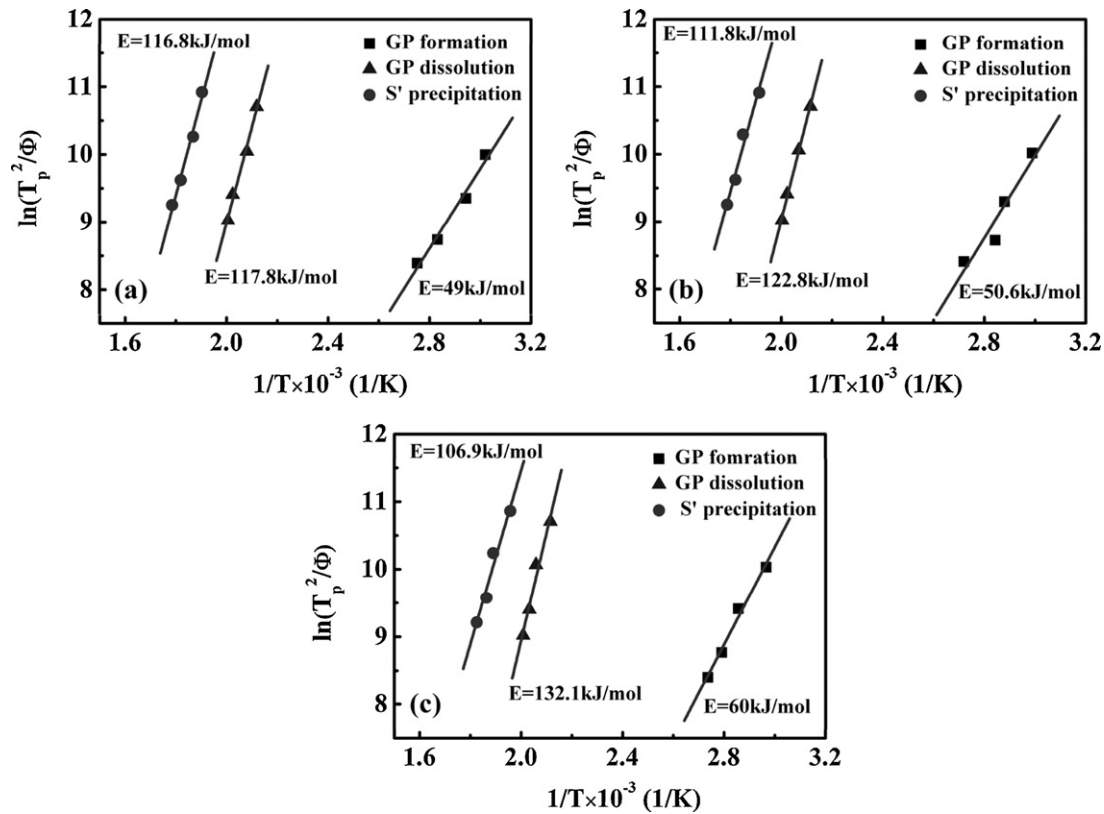| Solution temperature, °C	Activation energies, kJ/mol		
	GP formation	GP dissolution	S′ precipitation
495	49.1	117.8	116.8
530	50.6	122.8	111.8
560	60.0	132.1	106.9

Fig. 9. Variations of $\ln [T_p^2/\Phi]$ with $1/T_p$ for GP zone formation and dissolution, and S′ precipitation.

where B is a geometric constant that is theoretically between 4 (when the reinforcement aspect ratio = ∞) and 12 (when the reinforcement aspect ratio = 1), V_f is the volume fraction of reinforcements, b is the Burgers vector and t is the smallest dimension of the reinforcements.

The higher the value of ΔT, the greater the residual stress, and the greater the dislocation density formed in the matrix [31]. Oguocha thought that when the cooling rate exceeded a certain critical value, the concentration of quenched in vacancies would decrease because of the higher probability of vacancy annihilation at dislocations [32]. Hence, the vacancy concentration is lower and the peak temperature for the GP zone formation is higher for the composite solutionized at a higher temperature. This suggests that the GP zone formation requires a higher driving force for the composite with a higher solution temperature. This is consistent with variation in the activation energy with the solution temperature as shown in Table 3.

The values of the activation energy for the GP zone dissolution of the composites are determined to be from 117.8 to 132.1 kJ/mol for the solution temperatures from 495 to 560 °C. The activation energy for the solute diffusion during the GP zone dissolution process includes the activation energies for the formation of excess vacancies and for the solute transport. This implies a higher effective activation energy for the GP zone dissolution in a vacancy-deficient environment than that in a vacancy-rich environment [33]. Therefore, the effective activation energy for the GP dissolution in the composite with a higher solution temperature is larger than that with a lower solution temperature.

Table 3 shows that the thermal diffusion activation energy for the S′ phase formation in the composites is from 116.8 to 106.9 kJ/mol for the solution temperatures from 495 to 560 °C. Obviously, the thermal diffusion activation energy in the composite decreases as the solution temperature increases. That is to say, the precipitation of the S′ phase was accelerated at higher

solution temperatures. This resulted in the accelerated aging kinetics of the composites with increasing the solution temperature. Nieh and Karlak [34] attributed the reduction in the activation energy for diffusion in the composites to enhanced solute diffusion along dislocations to the growing transition precipitates. Dong et al. [35] thought that the high density of dislocations in the SiCw/Al–Li–Cu–Mg–Zr composite can provide additional heterogeneous nucleation sites for the S′ phase, especially in the early stage of aging. Nucleating of the S′ phase on dislocations significantly reduced the critical energy for nucleation, resulting in accelerated precipitation of the S′ phase.

3.3. Mechanical properties

The mechanical properties of the peak-aged composites solutionized at various temperatures are given in Table 4. It is noted that the composite solutionized at 530 °C exhibited the highest strength and elongation. However, the strength increment is slight. This variation trend is consistent with that of the peak hardness, as shown in Table 1. In the previous studies [22,23], the effect of the solution temperature on the mechanical properties of the 15 vol.%SiCw/2024Al–T6 and 17.8vol.%SiCp/2124Al–T4 composites was investigated. It was reported that the SiCw/2024Al and SiCp/2124Al composites exhibited significantly enhanced strength

Table 4
Tensile properties of SiCp/2009Al composite at peak aging condition with different solution temperatures.

Solution temperature, °C	Yield strength, MPa	Tensile strength, MPa	Elongation to fracture, %
495	365	495	7.2
530	375	500	7.6
560	365	490	4.0

and elongation for the optimum solution temperature of 540 and 545 °C, respectively. This property enhancement was attributed to the dissolution of intermetallics containing Cu, Mg and/or Mn, which reduced the possibility of premature particle fracture and increased the solution strengthening and aging strengthening, and the increase in the dislocation density [22,23].

For the present $SiC_p/2009Al$ composite, the 2009Al was designed to contain only alloying elements Cu and Mg without other alloying elements such as Mn and impurity elements such as Si and Fe. The Fe associated with the Al_7Cu_2Fe phase is believed to come from the contamination during the blending of the powders. In this case, only a very small amount of intermetallics Al_2Cu and Al_7Cu_2Fe phase remained after the solution treatment, and no other types of intermetellics were detected. Therefore, the slight increase in the strength and hardness of the composite for the solution temperature of 530 °C should be attributed to the following factors. First, increasing the solution temperature from 495 to 530 °C resulted in a slight increase in the intermetellic dissolution (Fig. 2). This leads to a limited increase in the strength and hardness. Second, the higher quenching temperature produced a higher density of dislocations, thereby increasing the strength of the composite, as suggested by Ma et al. [22,31] and Thomas and King [23]. Third, the increase in the dislocation density enhanced the formation of the S′ precipitate at the dislocations through heterogeneous nucleation, increasing the strength of the composite. As reported by Thomas and King [23], the significant dissolution of intermetallics was the main factor increasing the strength of the composite at higher solution temperatures. In this study, the quantity of intermetallics was relatively low according to the composition design of the 2009Al matrix alloy. Therefore, the dissolution of intermetallics only exerted a limited effect on the strength of the composite. The comprehensive effect of these three factors results in a slight increase in the strength of the composite at a solution temperature of 530 °C. At higher solution temperature, the mechanical properties of the composite decrease due to the limited incipient melting around SiC interfaces [23].

4. Conclusions

From the analysis on the precipitation process of $SiC_p/2009Al$ composite, the following conclusions can been made:

1. With increasing the solution temperature from 495 to 560 °C, the amount of undissovled second-phase particles decreased, but the grain size increased.
2. The aging kinetics of the composite, solutionized at different temperatures, was accelerated compared to the unreinforced matrix alloy, and enhanced with increasing the solution temperature from 495 to 560 °C.
3. With increasing the solution temperature, the GP zone formation and dissolution were retarded due to the decreased quenched-in vacancy concentration, however, the S′ precipitation was accelerated due to the increased dislocation density.
4. At the solution temperature of 530 °C, the composite exhibited the highest hardness and strength. However, the strength increment was slight.

References

[1] D. Aidun, P. Martin, J. Sun, J. Mater. Eng. Perform. 1 (1992) 615–624.
[2] P.M. Singh, J.J. Lewandowski, Metall. Trans. A 24 (1993) 2531–2543.
[3] H.R. Shakeri, Zhirui Wang, Metall. Mater. Trans. A 33 (2002) 1699–1713.
[4] M. Zhao, G.H. Wu, L.T. Jiang, J. Mater. Sci. 39 (2004) 1759–1763.
[5] G.M. Janowski, B.J. Pletka, Metall. Mater. Trans. A 26 (1995) 3027–3035.
[6] V.K. Varma, Y.R. Mahajan, V.V. Kutumbarao, Scr. Mater. 37 (1997) 485–489.
[7] S.M.R. Mousavi Abarghouie, S.M. Seyed Reihani, Mater. Des. 31 (2010) 2368–2374.
[8] P. Appendino, C. Badini, F. Marino, A. Tomasi, Mater. Sci. Eng. A 135 (1991) 275–279.
[9] M.P. Thomas, J.E. King, J. Mater. Sci. 29 (1994) 5272–5278.
[10] J.M. Papazian, Mater. Trans. A 19 (1988) 2945–2953.
[11] A. Daoud, W. Reif, J. Mater. Process. Tech. 123 (2002) 313–318.
[12] S. Suresh, T. Christman, Y. Sugimura, Scr. Metall. 23 (1989) 1599–1602.
[13] R.J. Arsenault, N. Shi, Mater. Sci. Eng. 81 (1986) 175–187.
[14] K.K. Chawla, A.H. Esmaeili, A.K. Datye, A.K. Vasudevan, Scr. Metall. Mater. 25 (1991) 1315–1319.
[15] T.S. Kim, T.H. Kim, K.H. Oh, H.I. Lee, J. Mater. Sci. 27 (1992) 2599–2605.
[16] S.I. Hong, G.T. Gray III, Acta Metall. Mater. 40 (1992) 3299–3315.
[17] Sharmilee Pal, R. Mitra, V.V. Bhanuprasad, Mater. Sci. Eng. A 480 (2008) 496–505.
[18] K.C. Chen, C.G. Chao, Metall. Mater. Trans. A 26 (1995) 1035–1043.
[19] W. Li, J.P. Long, S. Jing, B.L. Shen, S.J. Gao, M.J. Tu, J. Mater. Eng. Perform. 12 (2003) 19–22.
[20] H.K. Ahn, C.H. Yu, Met. Mater. Int. 7 (2001) 1–7.
[21] I. Dutta, D.L. Bourell, Mater. Sci. Eng. A 112 (1989) 67–77.
[22] Z.Y. Ma, Y.X. Lü, M. Lou, J. Bi, J. Mater. Sci. Technol. 11 (1995) 291–294.
[23] M.P. Thomas, J.E. King, Compos. Sci. Technol. 56 (1996) 1141–1149.
[24] I. Özbek, Mater. Charact. 58 (2007) 312–317.
[25] P. Rodrigo, P. Poza, V. Utrilla, A. Ureña, J. Alloys Compd. 479 (2009) 451–456.
[26] R.D. Schueller, A.K. Sachdev, F.E. Wawner, Scr. Metal. Mater. 27 (1992) 617–622.
[27] R.D. Schueller, A.K. Sachdev, F.E. Wawner, Metal. Mater. 27 (1992) 1289–1294.
[28] P. Rodrigo, P. Poza, M.V. Utrilla, A. Ureña, J. Alloys Compd. 482 (2009) 187–195.
[29] G.W. Smith, W.J. Baxter, R.K. Mishra, J. Mater. Sci. 35 (2000) 3871–3880.
[30] D. Turnbull, R.L. Cormia, Acta Metall. 8 (1960) 747–750.
[31] Z.Y. Ma, J. Bi, Y.X. Lü, M. Lou, Y.X. Gao, Scr. Metal. Mater. 29 (1993) 225–229.
[32] I.N.A. Oguocha, M. Radjabi, S. Yannacopoulos, J. Mater. Sci. 35 (2000) 5629–5634.
[33] M.V. Rooyen, J.A.S. Maartensdijk, E.J. Mittemeijer, Metall. Trans. A 19 (1988) 2433–2443.
[34] T.G. Nieh, R.F. Karlak, Scr. Metall. 18 (1984) 25–28.
[35] S.L. Dong, J.F. Mao, D.Z. Yang, Y.X. Cui, L.T. Jiang, Mater. Sci. Eng. A 327 (2002) 213–223.